Charged Particle Distributions in DIS and Photoproduction at HERA

Daniel Traynor, ICHEP July 2010

Scaled Momentum Spectra in deep inelastic Scattering at HERA
(ZEUS, DESY-09-229 accepted by JHEP)

Observation of the Hadronic Final State Charge Asymmetry in High Q^2 Deep-Inelastic Scattering at HERA
(H1, Phys. Lett. B 681 (2009) 125)

Scaled momentum distributions of charged particles in dijet photoproduction at HERA
(JHEP08(2009)077)

Transverse Momentum of Charged Particles at low Q^2 at HERA
(H1prelim-10-035)

Motivation

- Tests of factorisation and the universality of fragmentation by
  - direct tests: Compare the same measurements (e.g. Fragmentation functions) from different experiments (Zeus, H1, CDF, OPAL, etc...) with each other.
  - Indirect tests: Compare a variety of measurements with the same theory (Monte Carlo, MLLA, NLO+FF). Monte Carlo and NLO Fragmentation function parameterisations fitted to e^+e^- annihilation data. MLLA parameters taken from global fit to all data.
- Non DGLAP behaviour of parton dynamics
  - Go to area of phase space that is expected to be sensitive to DGLAP / BFKL / CCFM differences (low Q2, low x DIS) and compare data to different model predictions.

HERA, ZEUS and H1

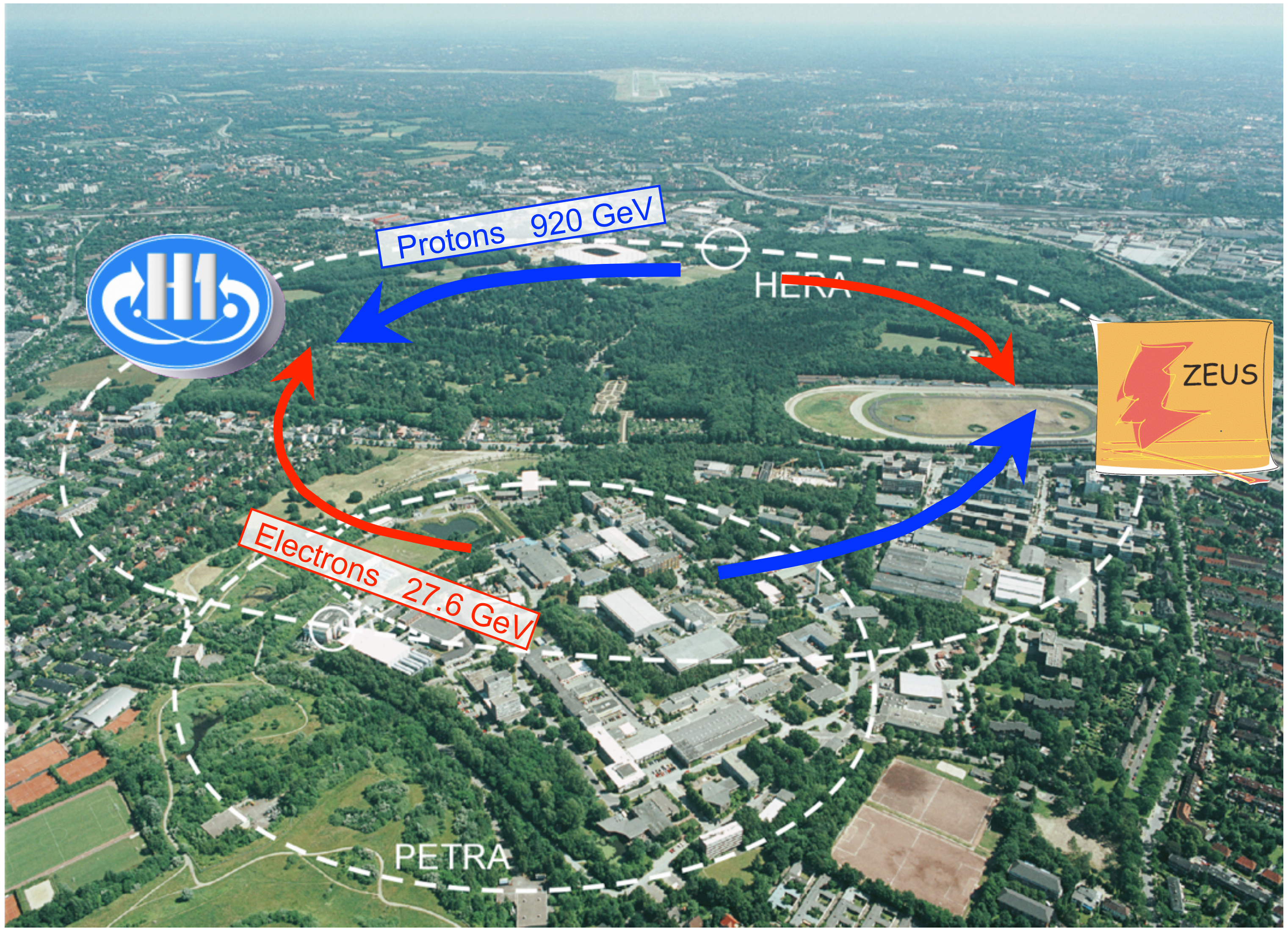

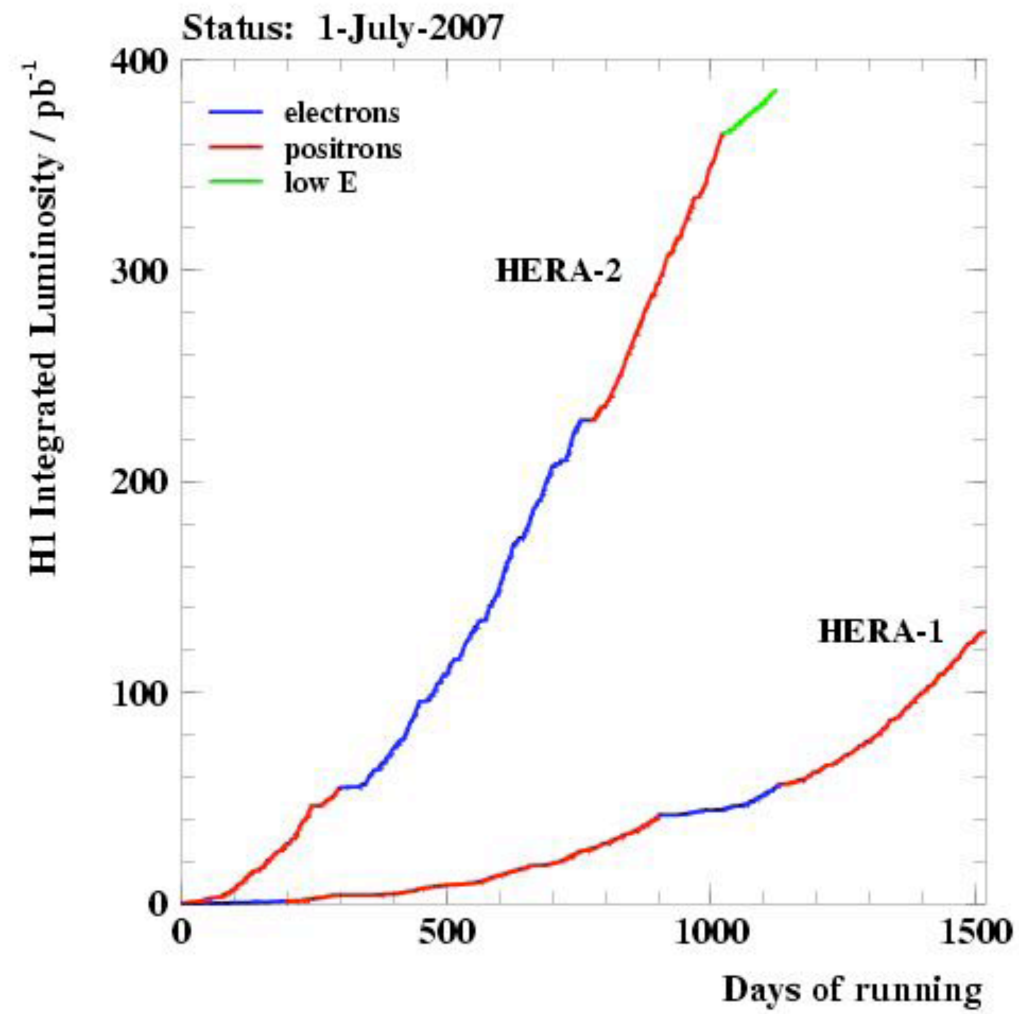

electrons and positrons

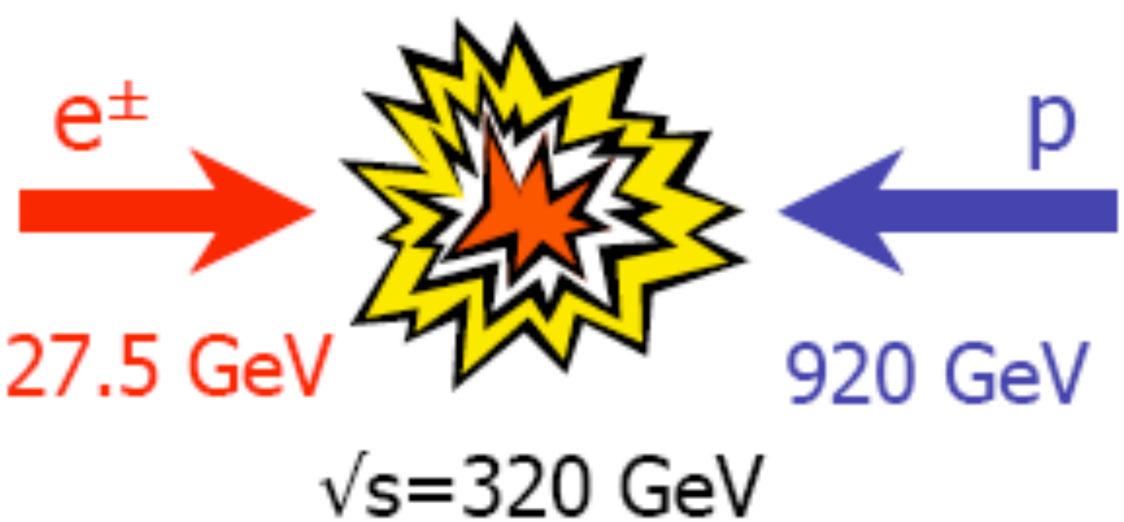

H1 and ZEUS are general purpose detectors with extensive tracking and calorimetry coverage

Usable luminosity per experiment ~500 pb^{-1}

Inclusive Deep Inelastic Scattering (DIS)

$Q^2 > 1$ GeV^2

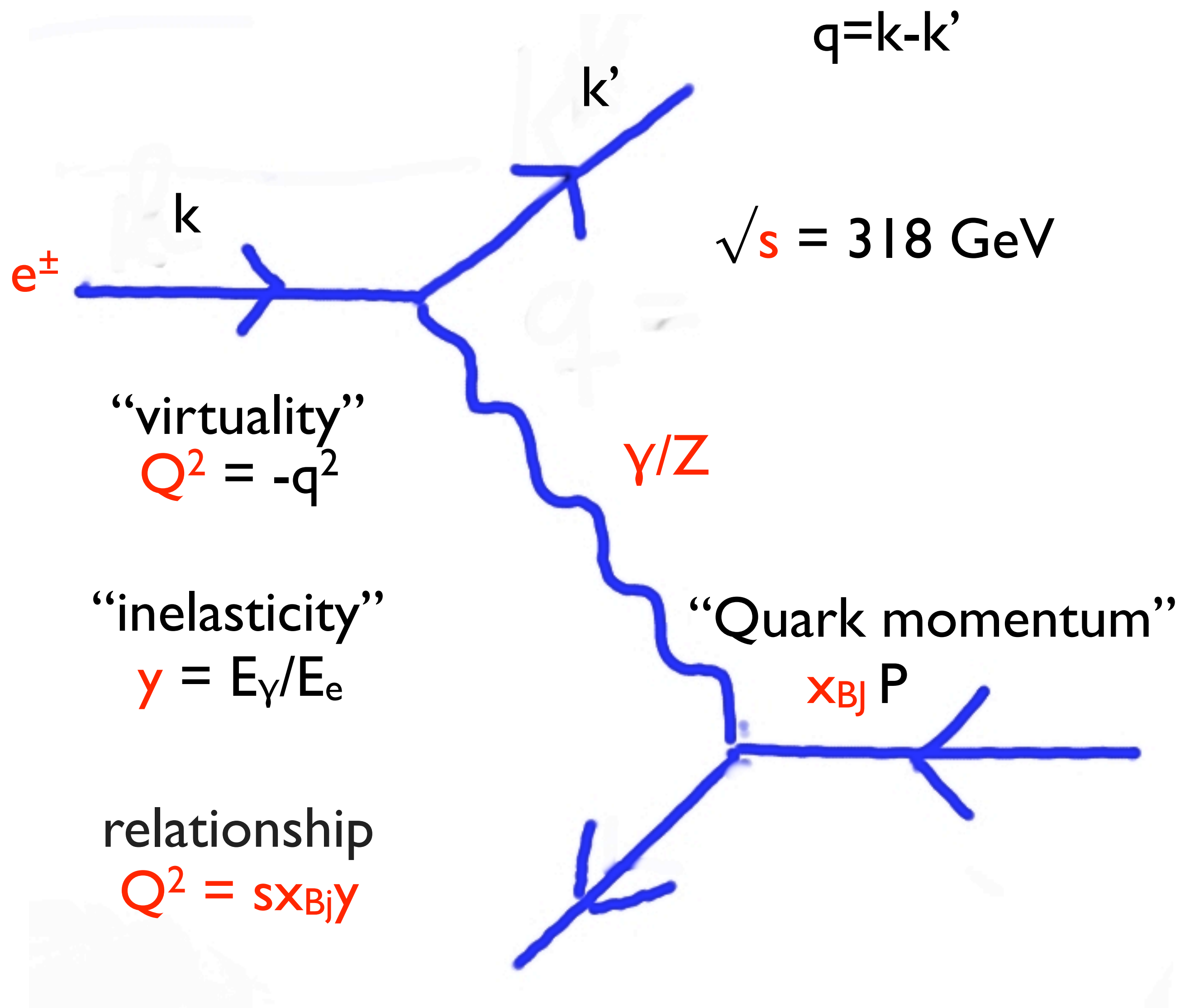

Dijet Photoproduction (γp)

$Q^2 \approx 0$ GeV^2

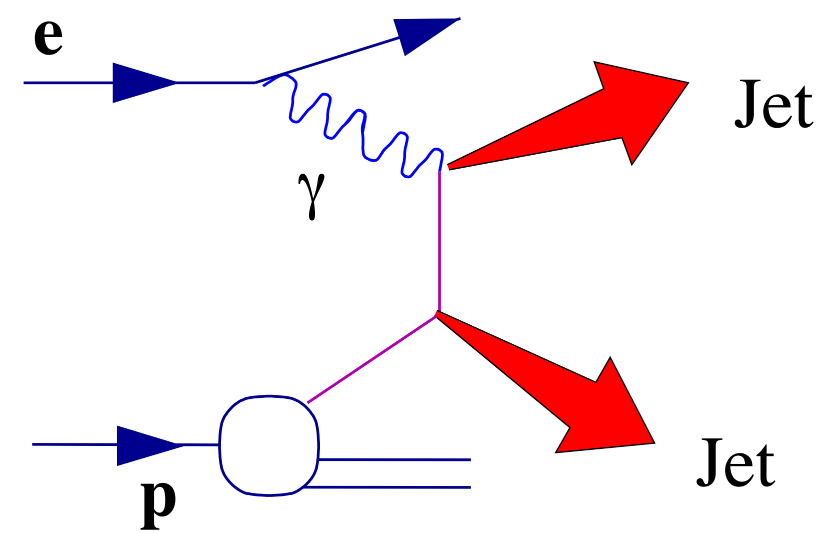

The dijet system used to characterises the event kinematics

Inclusive Deep Inelastic Scattering (DIS)

ep→eX $e^+e^-\to q\bar{q}$

Breit Frame

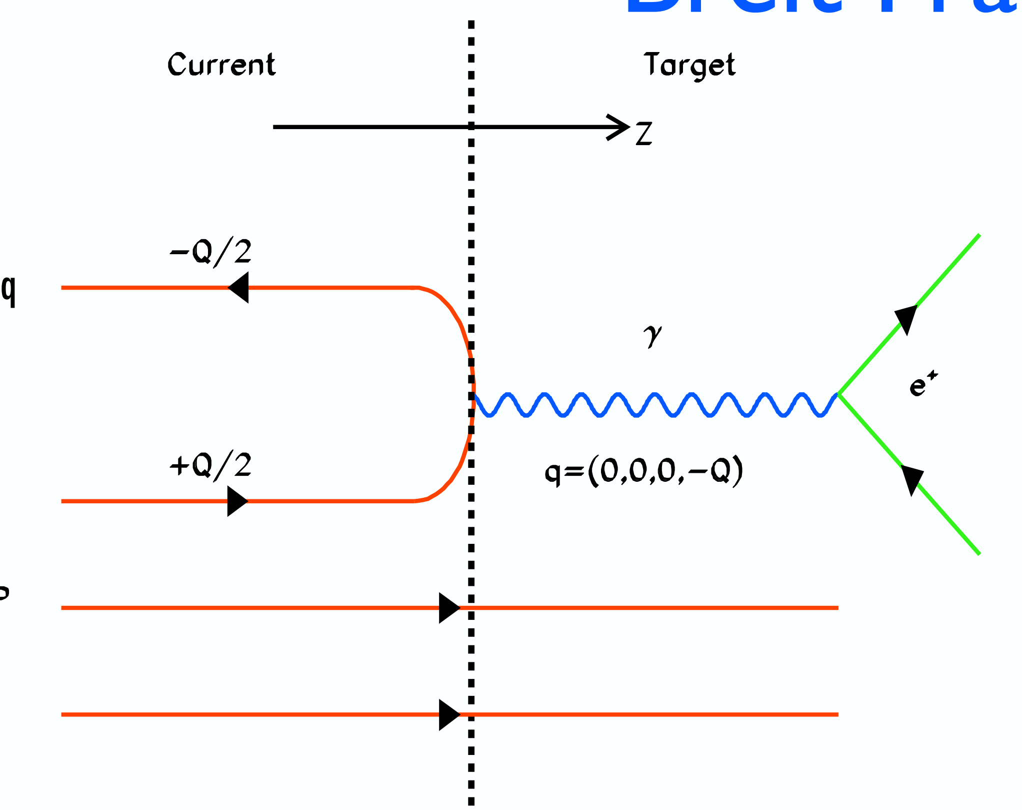

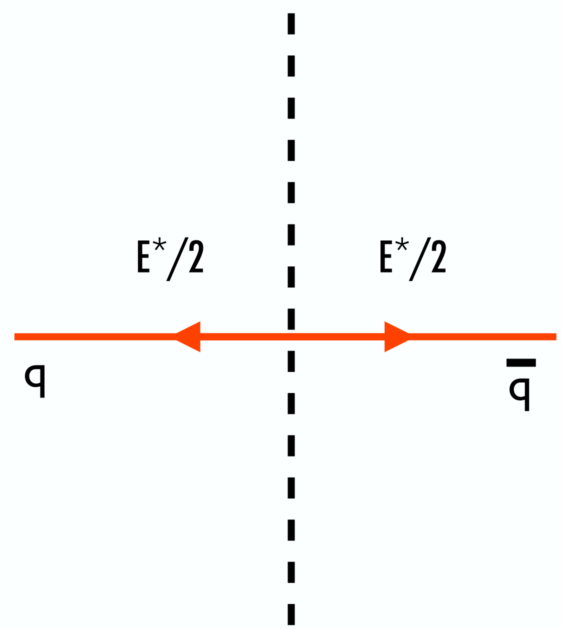

current region ≡ e^+e^- hemisphere

$$x_p = \frac{2P_h}{Q}$$

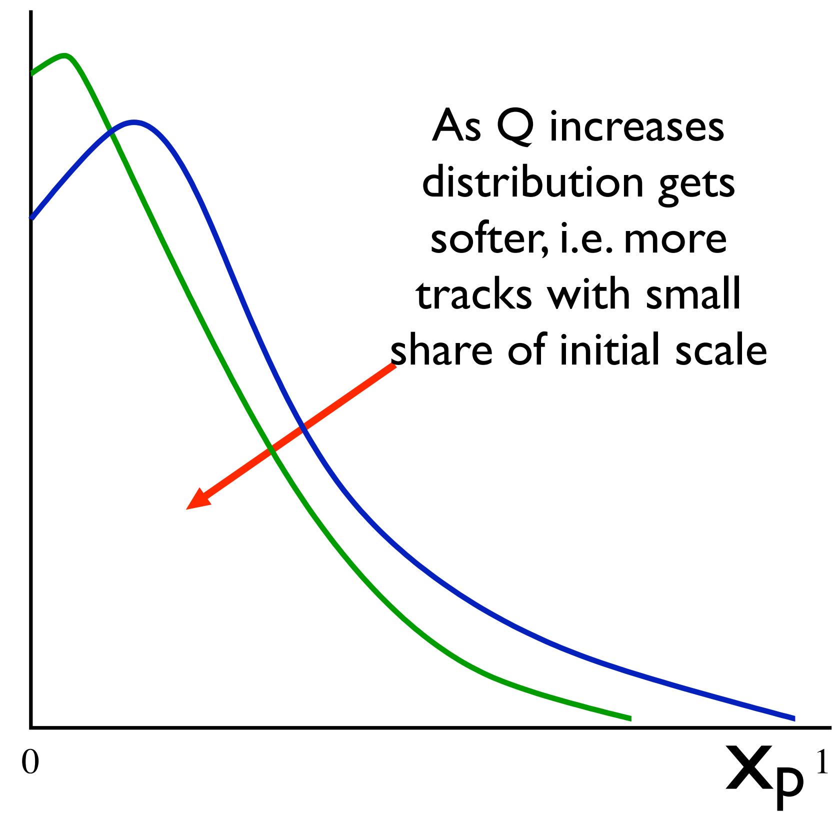

virtual photon doesn't carry any energy only longitudinal momentum (P_z)

Provides clearest separation between particles from hard scattering and proton remnant. Allows for easy comparison with e^+e^- data

x_p is the particle momentum in the Breit frame scaled by the energy scale in current region (Q/2).

Inclusive Deep Inelastic Scattering (DIS)

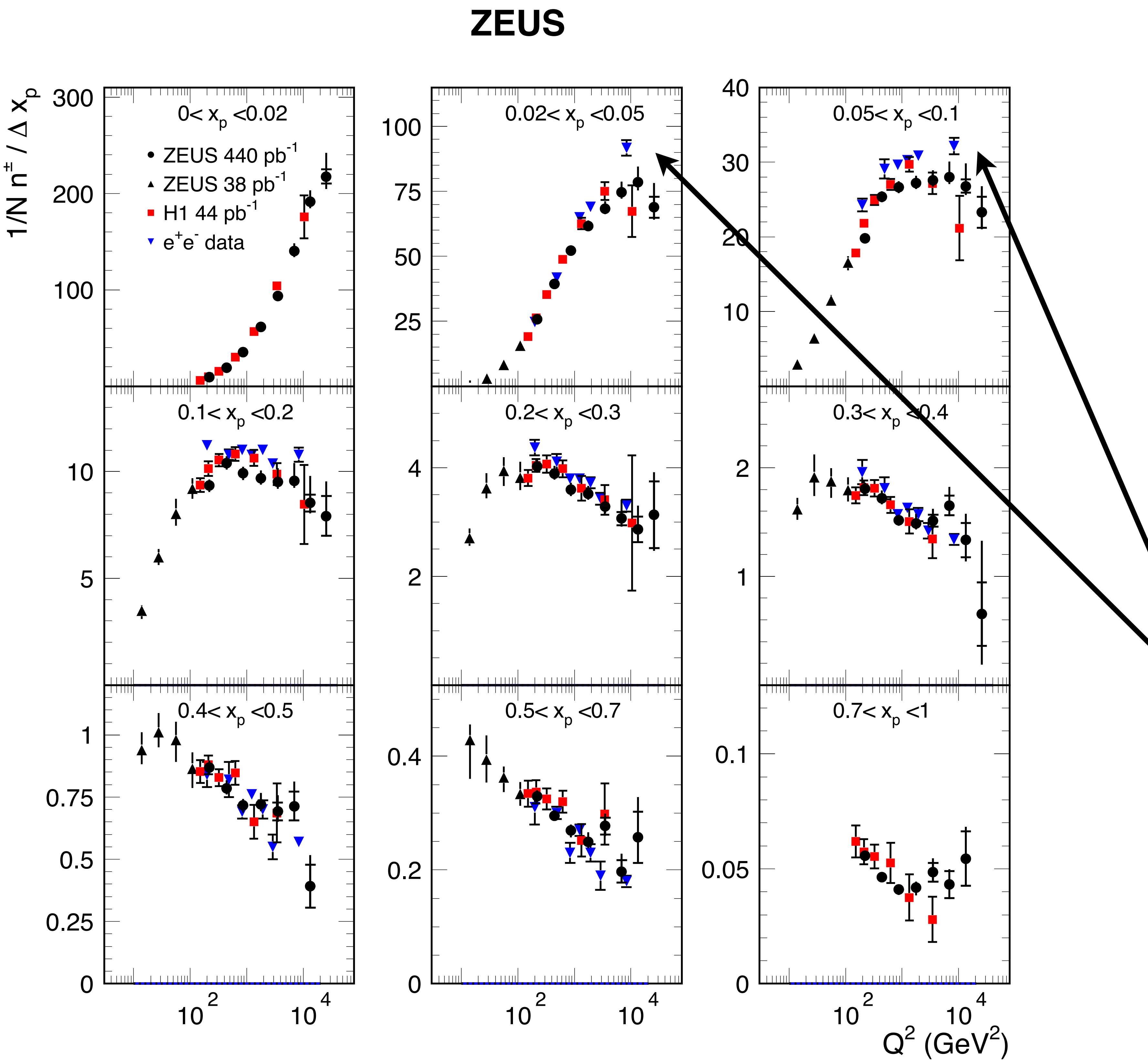

Data
$0.44\ fb^{-1}$
Event Selection
$10 < Q^2 < 41{,}000\ GeV^2$
$y > 0.04$
Detector Track Selection
$|\eta| < 1.75$
$p_{t,lab} > 0.15$ GeV

On the whole the comparison with H1 data and with e^+e^- results supports fragmentation universality

Significant differences at high Q^2 and low x_p between ep and e^+e^-.

Due to Breit frame boost ep experiments can measure the x_p spectra down to 0.

Inclusive Deep Inelastic Scattering (DIS)

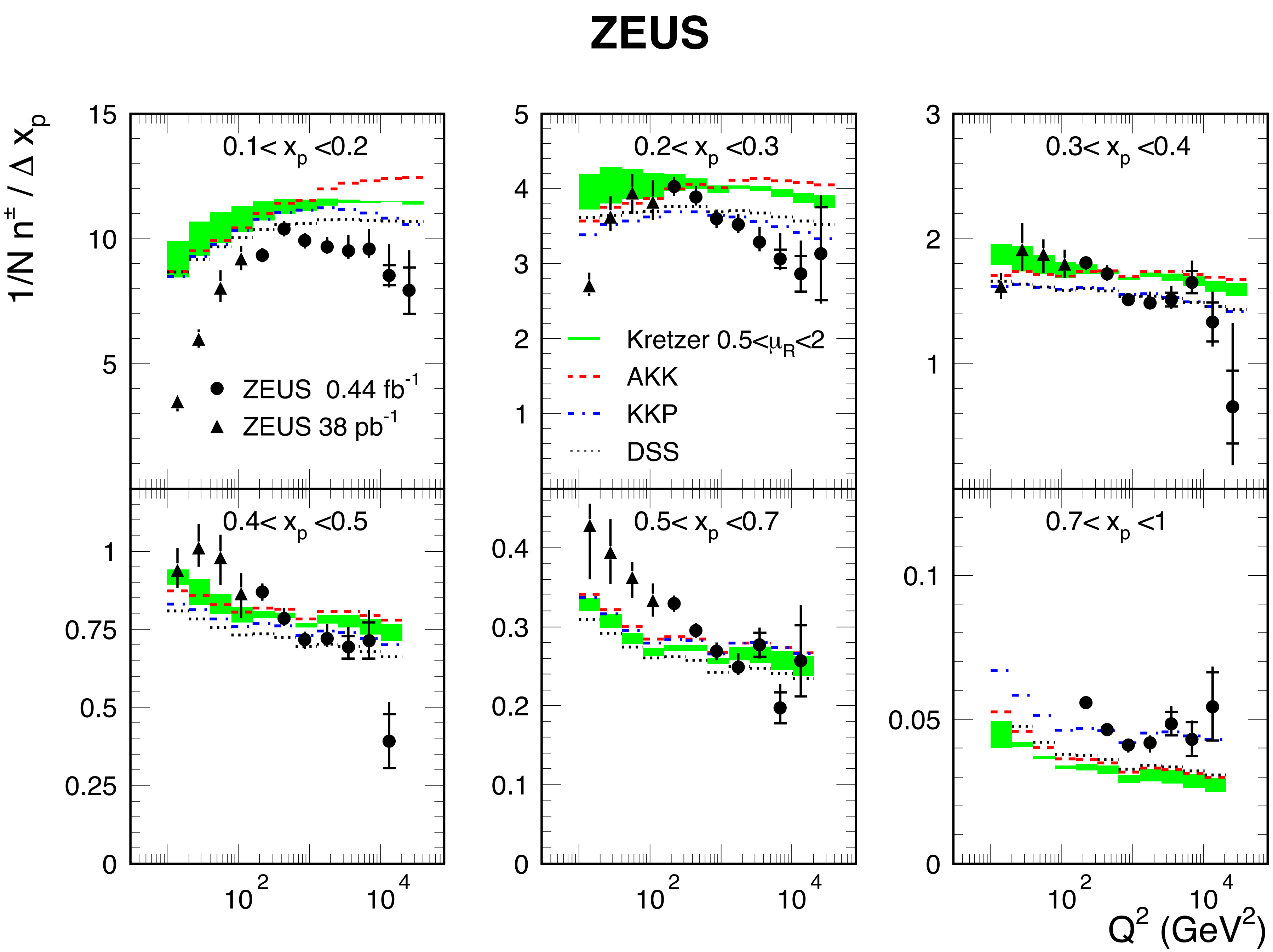

Full perturbative NLO QCD calculation combined with NLO Fragmentation functions which are parameterisations of e^+e^-.

NLO calculations do not provide a good description of the data.
Slope of the Q^2 dependence, scaling violation, are too small in theory!

Inclusive Deep Inelastic Scattering (DIS)

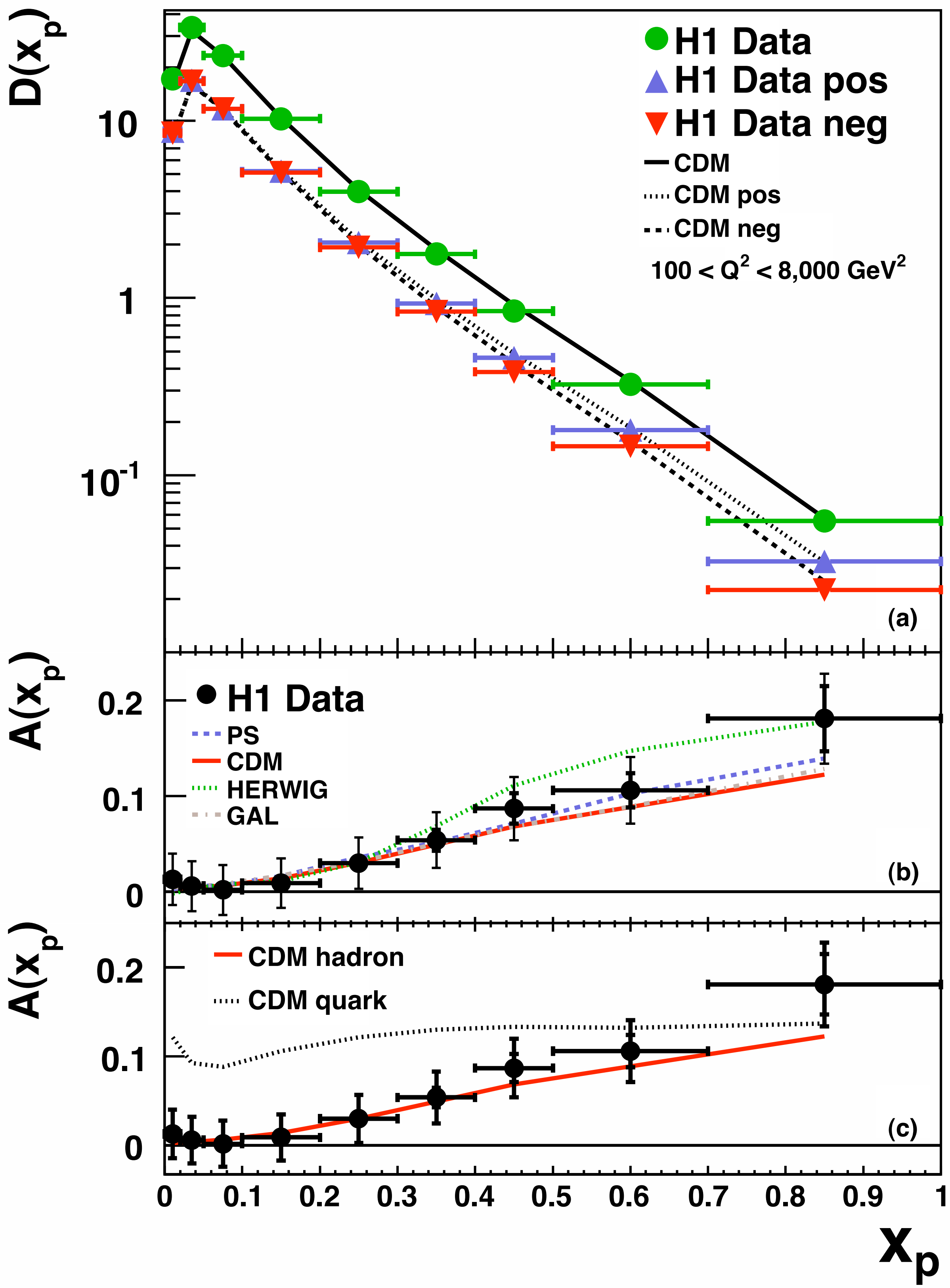

Fragmentation effects dominate at low x_p. Hadrons at large x_p expected come from the hard interaction.

At high Q^2 and high x_{BJ} significant contribution from valence quarks. Expect charge asymmetry in quarks from hard interaction.
Is it visible after hadronisation?

$$A(x_p) = \frac{D^+(x_p) - D^-(x_p)}{D(x_p)}$$

Charge asymmetry observed, increasing with x_p (also with Q^2, not shown)

Asymmetry described by Monte Carlo models

The results are consistent with the expectation that at high x_p the asymmetry is directly related to the valence quark content of the proton.

Dijet Photoproduction (γp)

Data

~23,000 events

L=359 pb^{-1}

Event Selection

$E_{TJet1,2} \geq 17$ GeV

$|\eta_{Jet1,2}| < 1.0$

$E_{TJet1}/E_{TJet2} \geq 0.8$

$0.9\pi \leq |\Phi_{Jet1}-\Phi_{Jet2}|$

$E_{TJet3} \leq 6$GeV

$|\eta_{Jet3}| \leq 2.4$

$0.2 \leq y \leq 0.8$

$Q^2 \leq 1$ GeV^2

$x_\gamma \geq 0.75$

Detecter Track Selection

$P_T \geq 0.15$ GeV

$|\eta| \leq 1.7$

Jets found with k_T algorithm, longitudinal invariant inclusive mode , R=1

Select back to back dijets, suppress 3rd jet. energy scale $E_{jet}= M_{jj}/2$

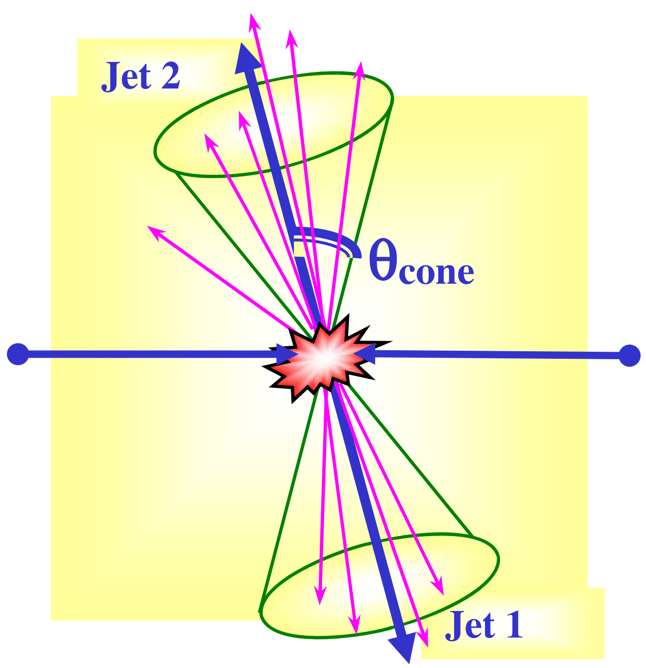

Fit the ξ distribution with; Gaussian around mean or full MLLA+LPHD theory.

Compare results from e^+e^-, ep, γp and $p\bar{p}$

$$\xi = ln(\frac{E_{jet}}{|p_{track}|})$$

Opening angle around jet axis (θ_c) links tracks to a particular jet (only results with θ_c = 0.23 considered here)

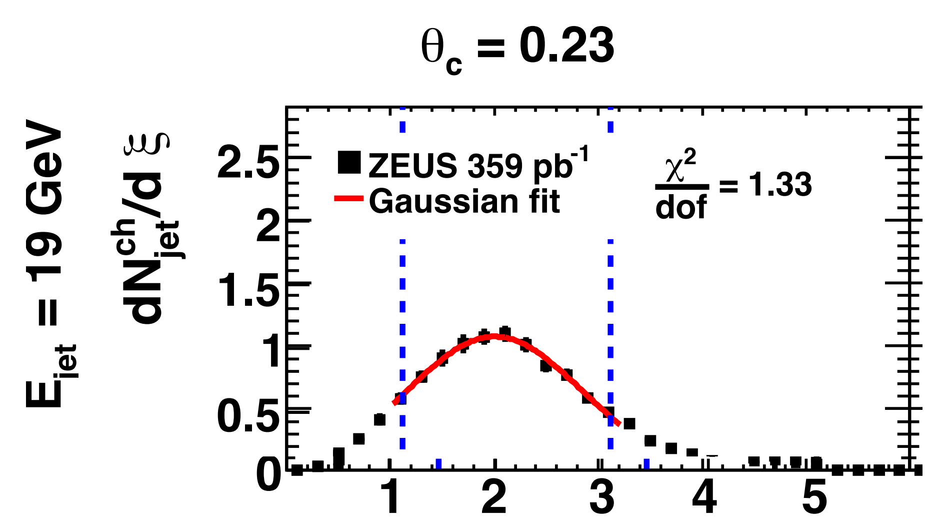

Tuesday, 13 July 2010

Dijet Photoproduction (γp)

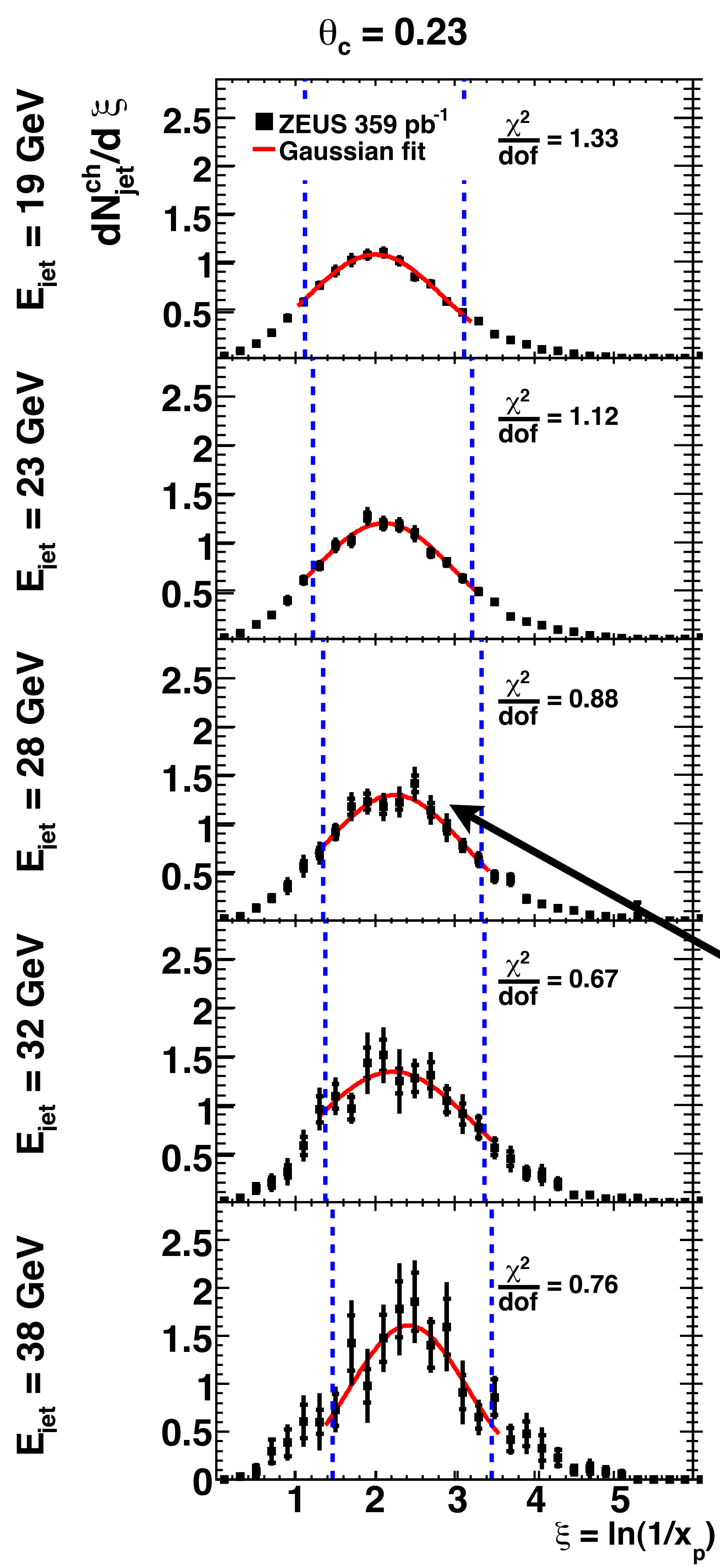

MLLA approximation to pQCD is a resummation approach where a subset of dominant terms in α_s are used to predict the shape of ξ

Λ_{eff} scale cut off independent of process considered!

κ_{ch} - normalisation factor to take into account fraction of neutral hadrons - independent of process considered

Fit Gaussian ± 1 around peak. For each E_{Jet} interval extract the peak position.

$$\Lambda_{eff} = \frac{E_{Jet} sin(\theta_c)}{\exp(\sqrt{0.87 + 2\xi_{peak}} - 0.54)^2} \quad \text{@LO}$$

or fit MLLA equation to all 5 energy points and extract Λ_{eff}

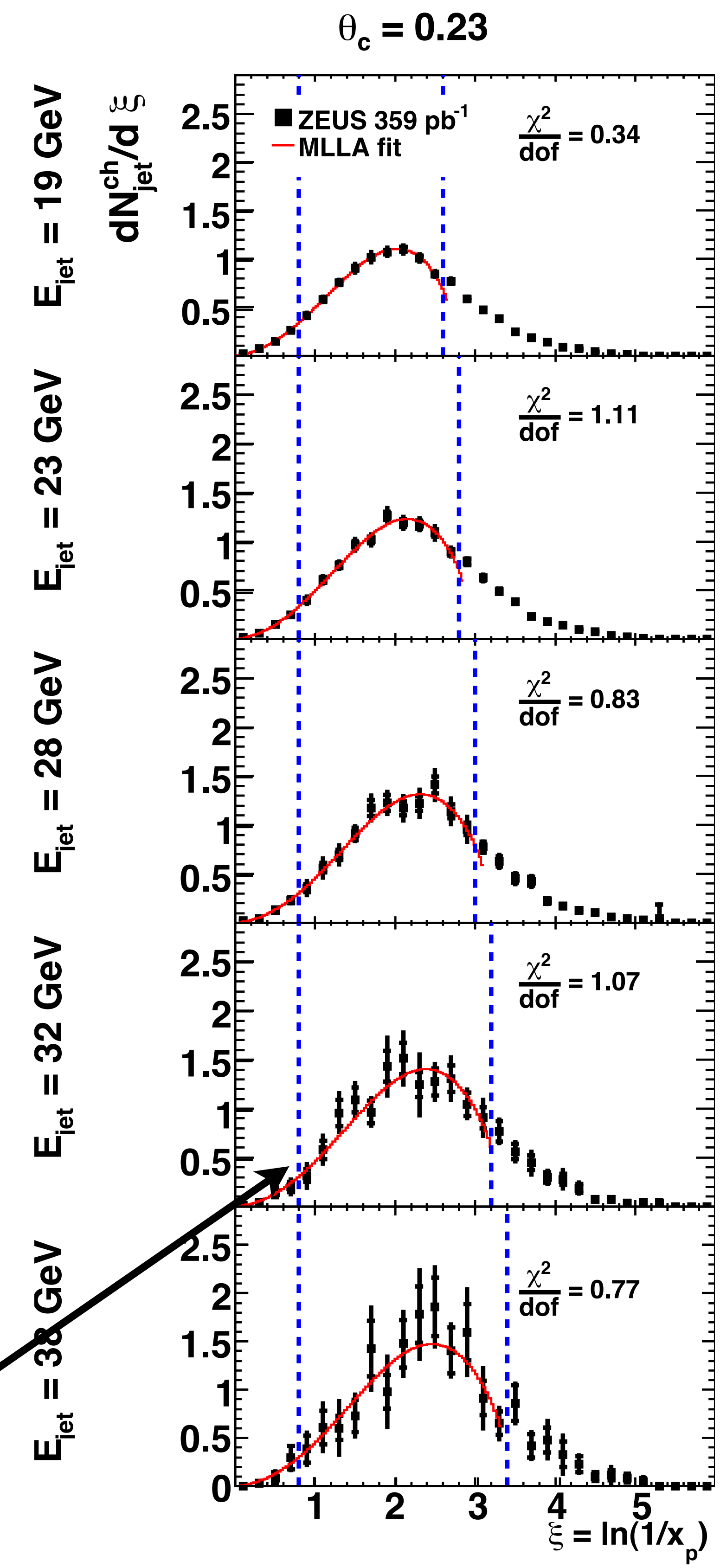

Dijet Photoproduction (γp)

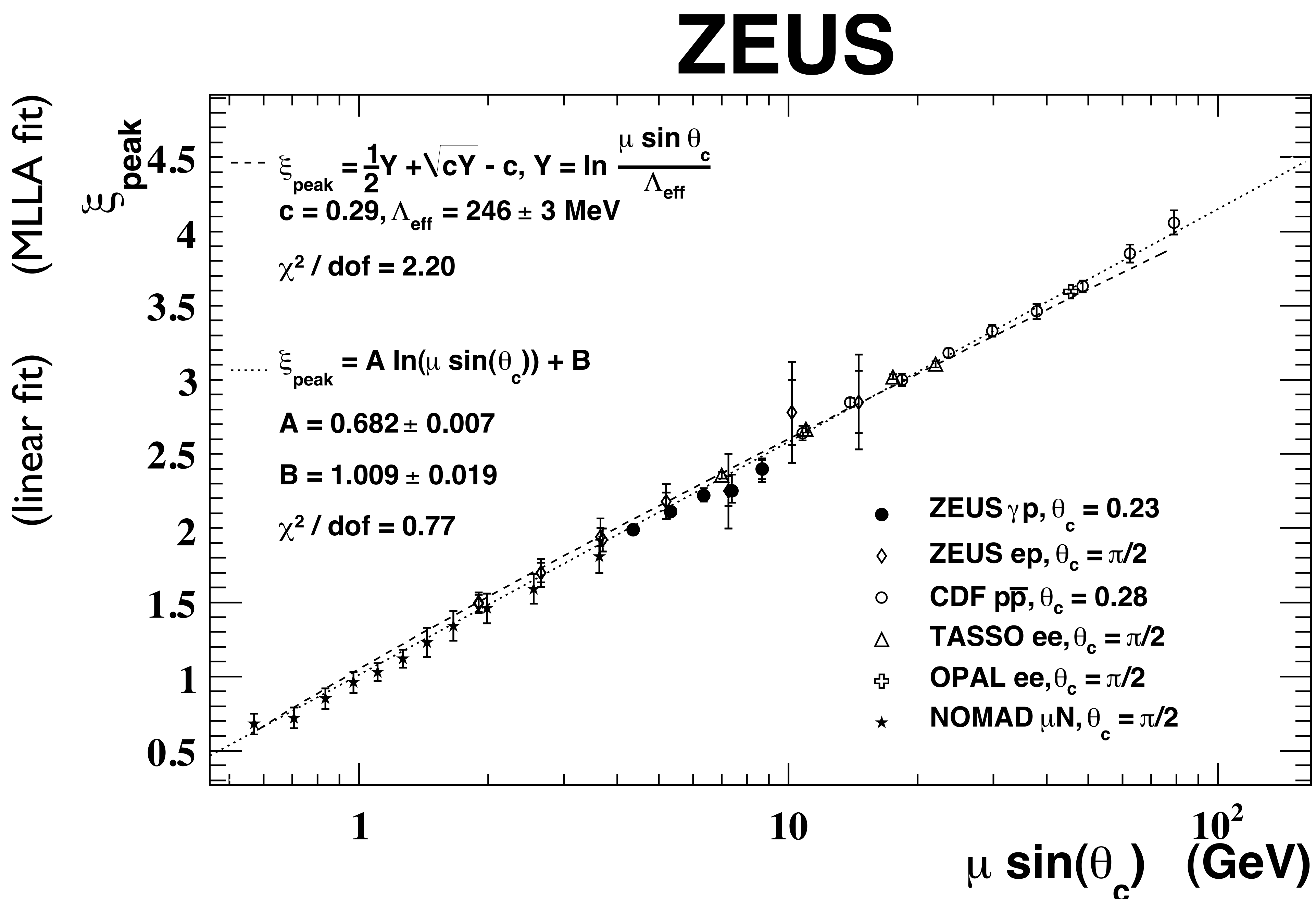

Characteristic energy scale = μ

Approximately linear relationship expected between ξ_{peak} and $\ln(\mu\sin(\theta_c))$

A linear fit using ZEUS data only produces a result that is consistent with the global fit to all data.

When MLLA theory is used to extract a value for Λ_{eff}, the extracted values of Λ_{eff} using only ZEUS data are not consistent with the global fit

θ_c : Opening angle around jet axis.

Dijet Photoproduction (γp)

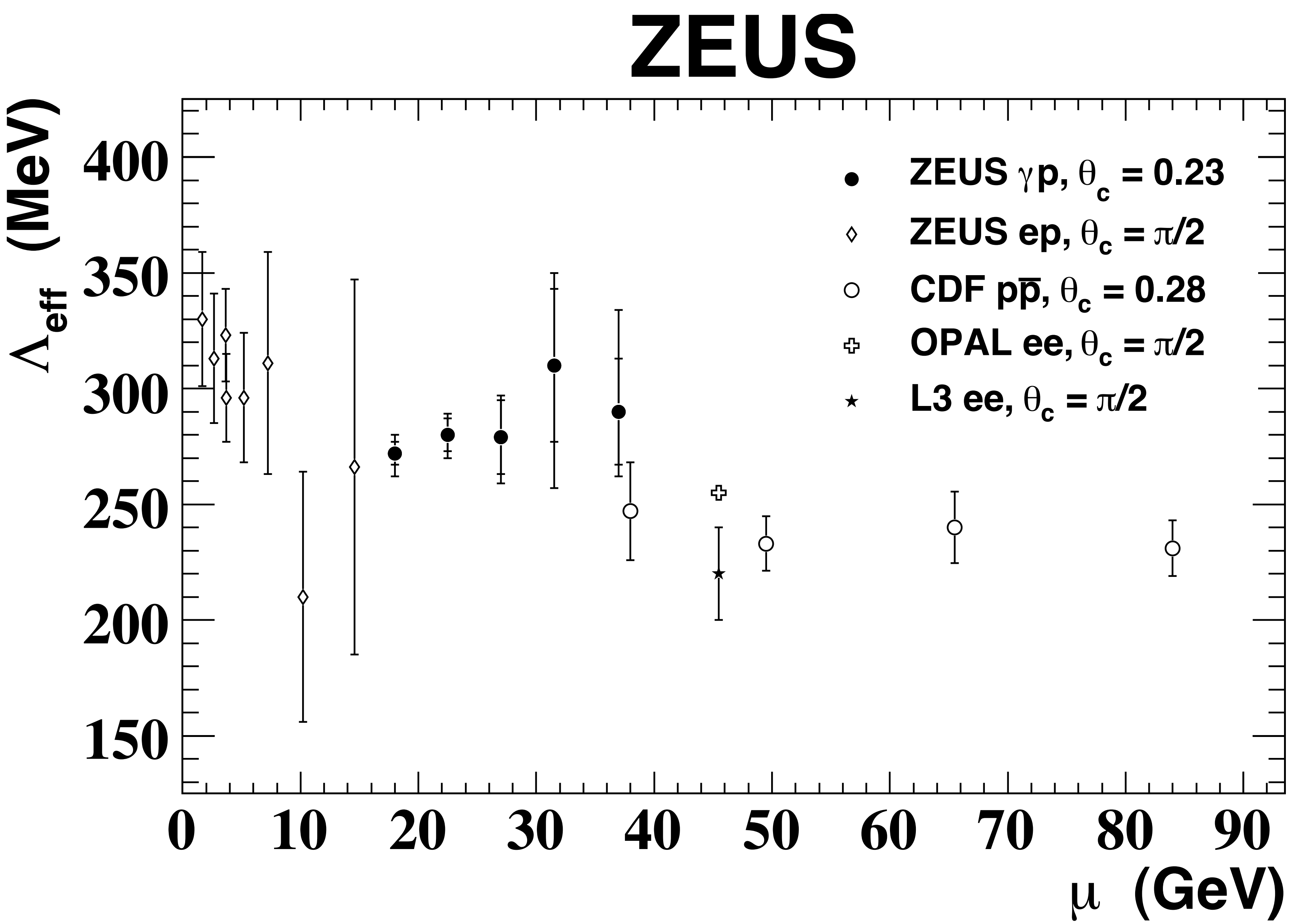

$$\xi_{peak} = \frac{1}{2}Y + \sqrt{cY} - c, \quad Y = \ln \frac{\mu \sin\theta_c}{\Lambda_{eff}}$$

Extract energy dependence of Λ_{eff} for data points

ZEUS γp data shows no dependence on μ, there is a small dependence on θ_c (not shown)

A weak dependence on μ and on θ_c is reported for the CDF data. This could explain the failure of global fit to to match ZEUS data only fit.

θ_c : Opening angle around jet axis.

Beyond DGLAP (DIS)

Data
2006 e^+p
$L = 88.6\ pb^{-1}$

Event Selection
$5 < Q^2 < 100\ GeV^2$
$0.05 < y < 0.7$

Detecter Track Selection
$p_T > 0.15$ GeV
$20° < \theta < 155°$

Measurement made in the hadronic centre of mass frame

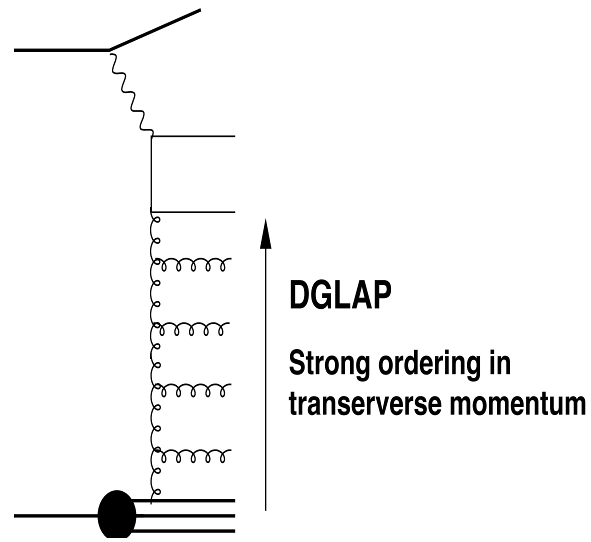

DGLAP: $Q_0^2 << k_{T1}^2 << ... << k_{Tn}^2 << Q^2$

Strong ordering in kT of emitted partons, works when Q^2 is large and x not too small. Implemented in RAPGAP Monte Carlo.

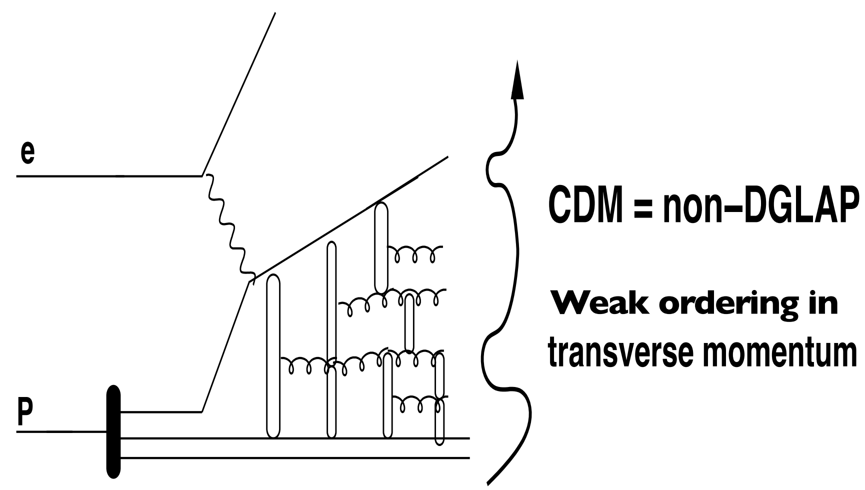

CDM (Colour Dipole Model): Produces weak ordering in parton k_T emission. Not evolution equation but gives BFKL like final state, works for small x. Used in DJANGOH Monte Carlo

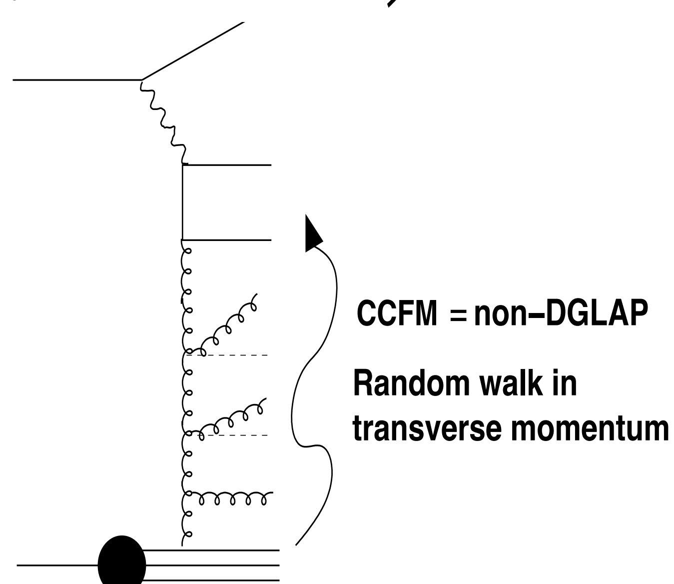

CCFM : random "walk" in k_T of emitted partons. Valid for both small and large x. Used in the CASCADE Monte Carlo.

Beyond DGLAP (DIS)

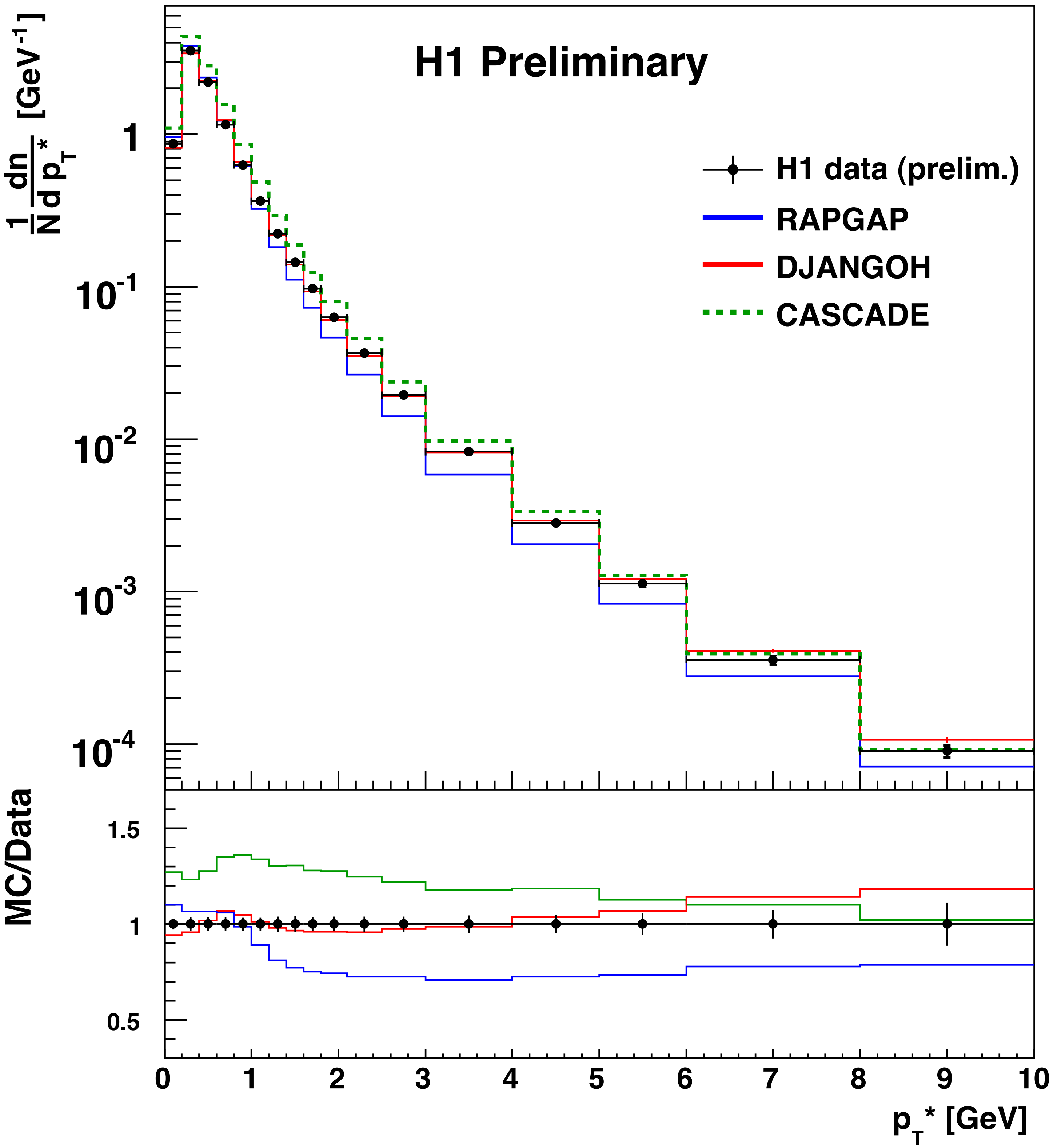

p_T^* in hadronic centre of mass frame

Djangoh (CDM) describes new data for whole p_T^* spectra.

Rapgap (DGLAP) is below the data $p_T^* > 1$GeV.

Cascade (CCFM) is systematically above the data.

Beyond DGLAP (DIS)

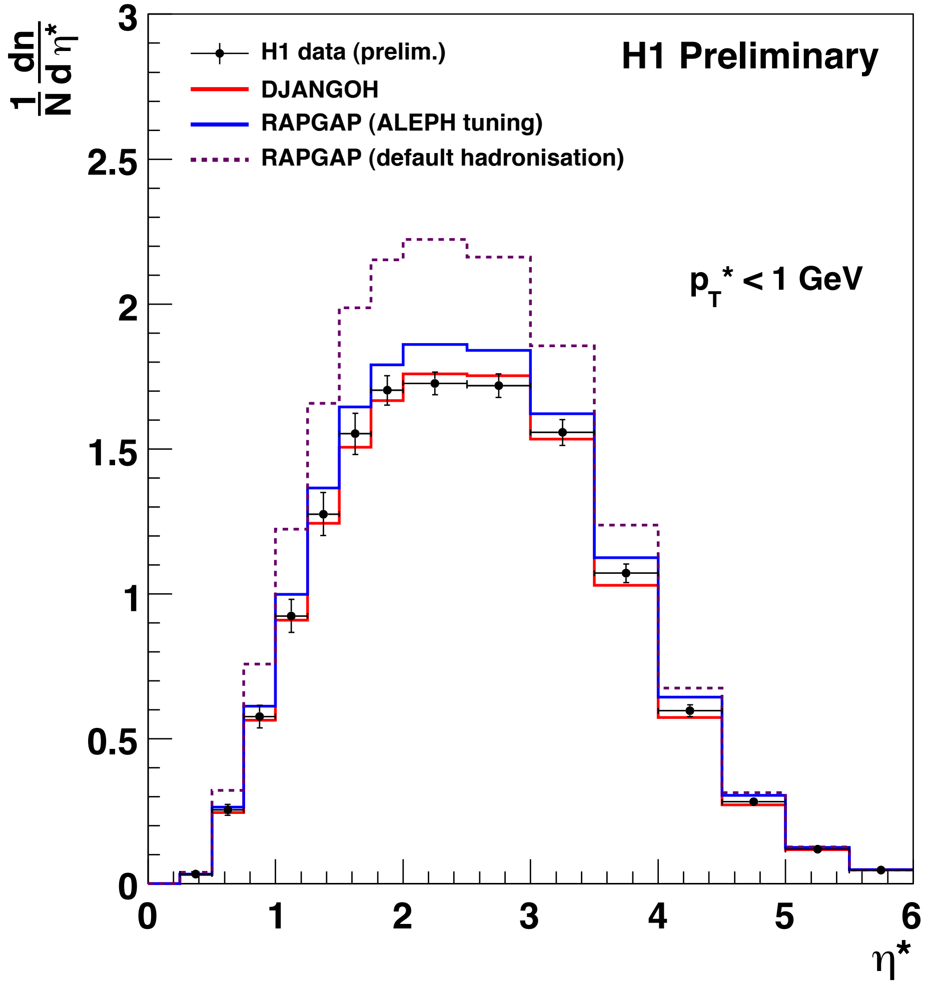

Charged particles with $p_T^* < 1$ GeV

Strong sensitivity to hadronisation parameters.

Weak sensitivity to different parton dynamics.

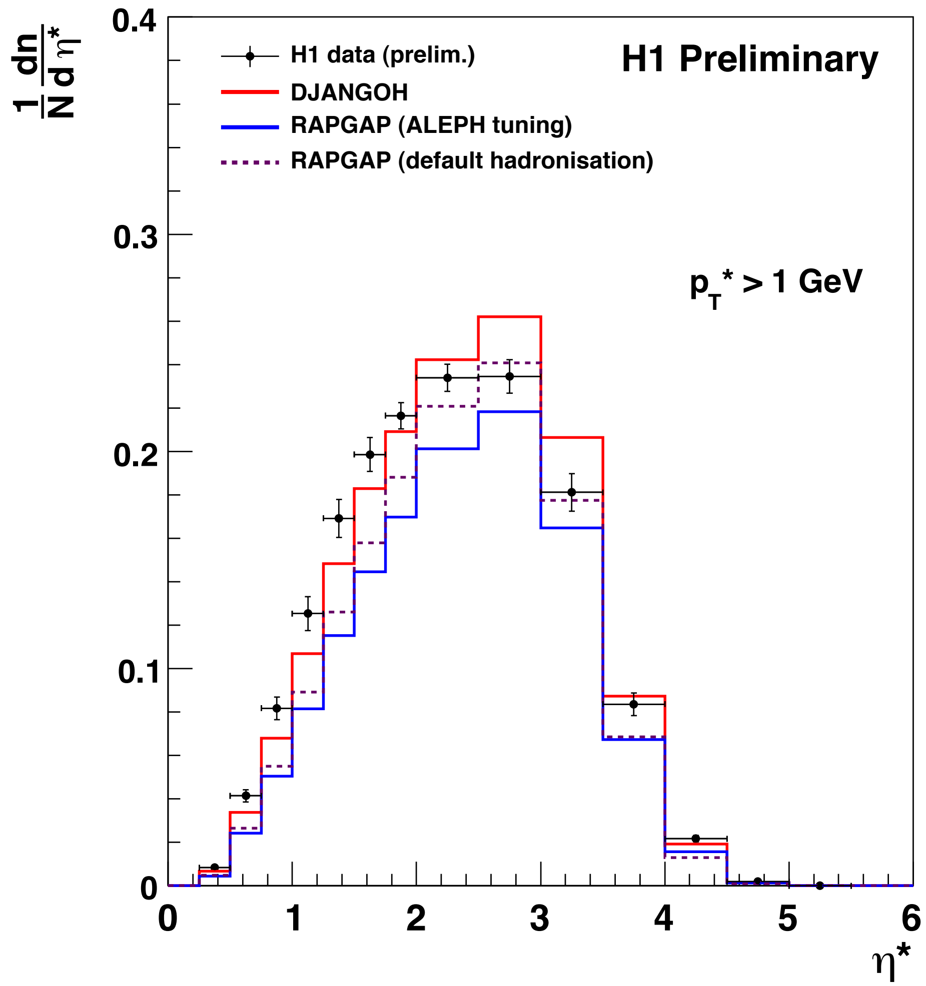

Charged particles with $p_T^* > 1$GeV

Weaker sensitivity to hadronisation parameters.

Stronger sensitivity to different parton dynamics.

η^* in hadronic centre of mass frame

Beyond DGLAP (DIS)

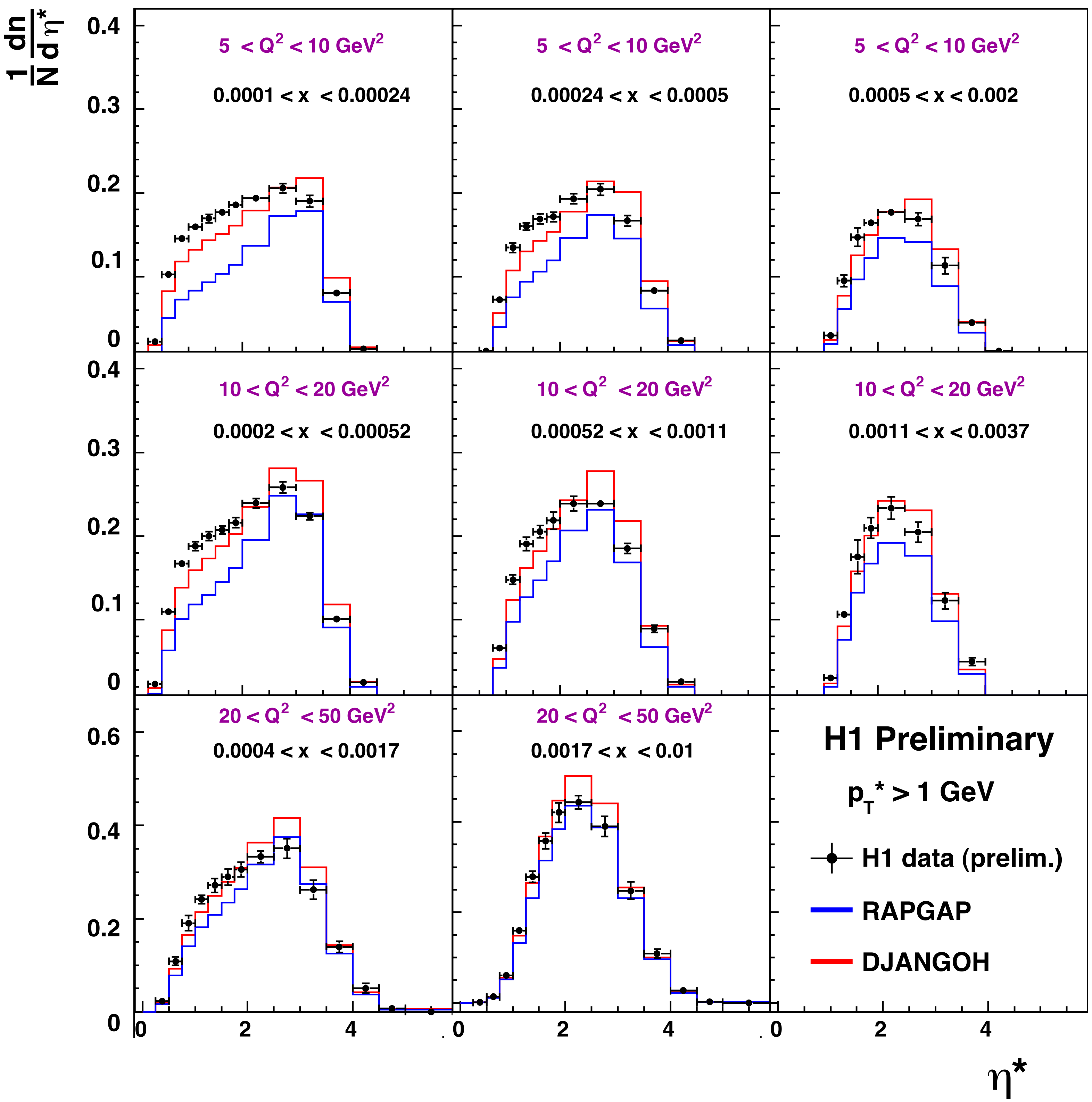

Charged particles with $p_T^* > 1$ GeV

Rapgap (DGLAP) is below the data for most of the phase space.

Djangoh (CDM) gives a better description of the data at low Q^2 and low x

η^* in hadronic centre of mass frame

Summary

- Charged particle spectra have been measured in DIS and photoproduction at HERA.
- In general the results are found to support the concept of quark fragmentation universality. However, there exists significant differences when comparing NLO QCD predictions to the data.
- The observed charge asymmetry is consistent with that expected from the valence quarks in the proton.
- At low x DIS, the CDM model is found to provide a better description of parton dynamics indicating that the emission of partons is not strongly ordered in k_T.

Backup

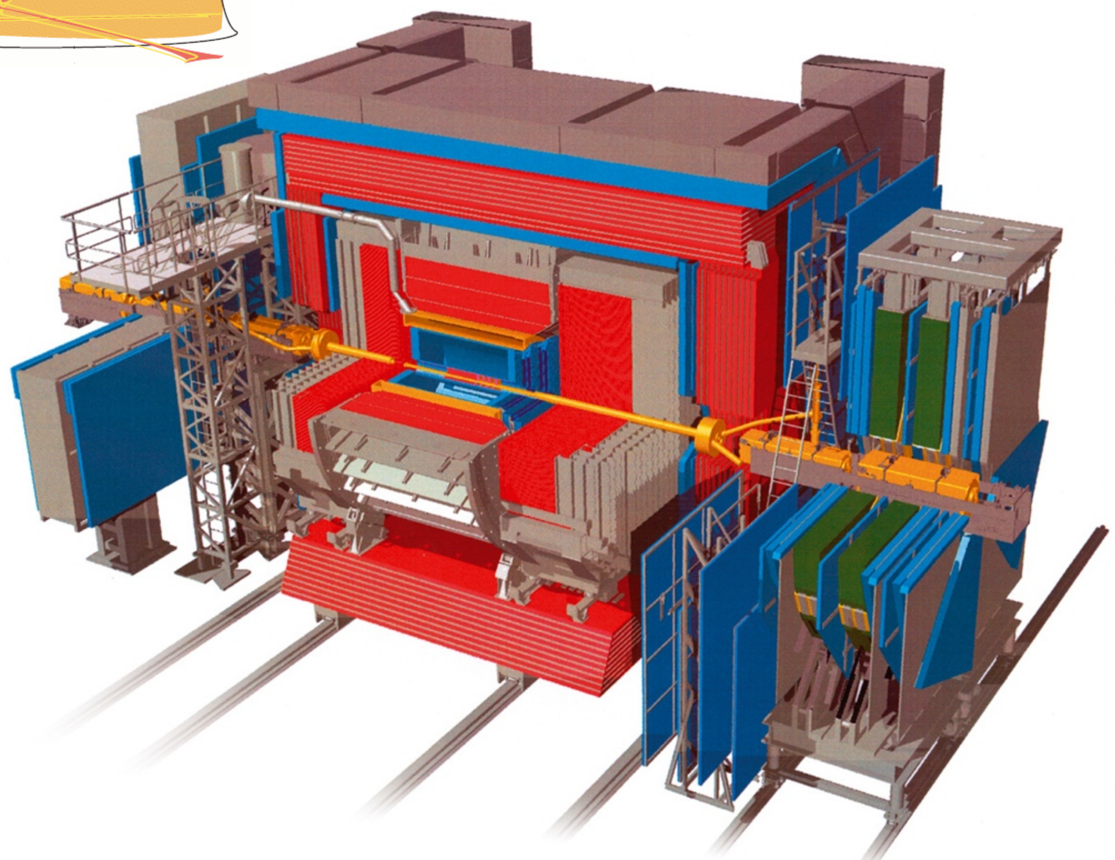

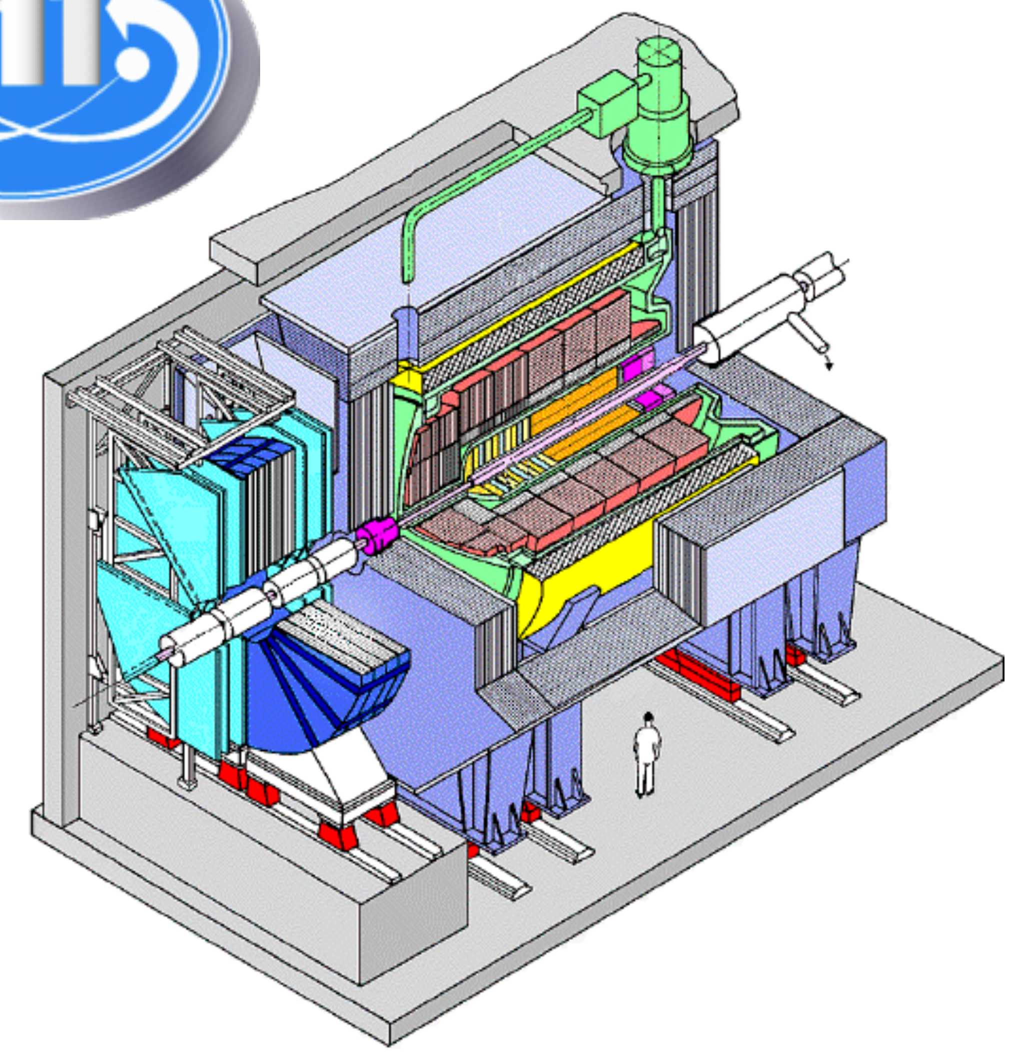

Central Tracking Detector
15° < θ < 164°
microvertex detector
7° < θ < 150°

Uranium Scintillator Calorimeter
(Electromagnetic and Hadronic)
2.2° < θ < 176.5°

Central Drift Chamber
20° < θ < 165°
silicon vertex detector
30° < θ < 150°

LAr Calorimeter
-1.4 < η < 3.4 convert to angle!
SpaCal Calorimeter
153° < θ < 178°

Frame of reference

LAB

Born level

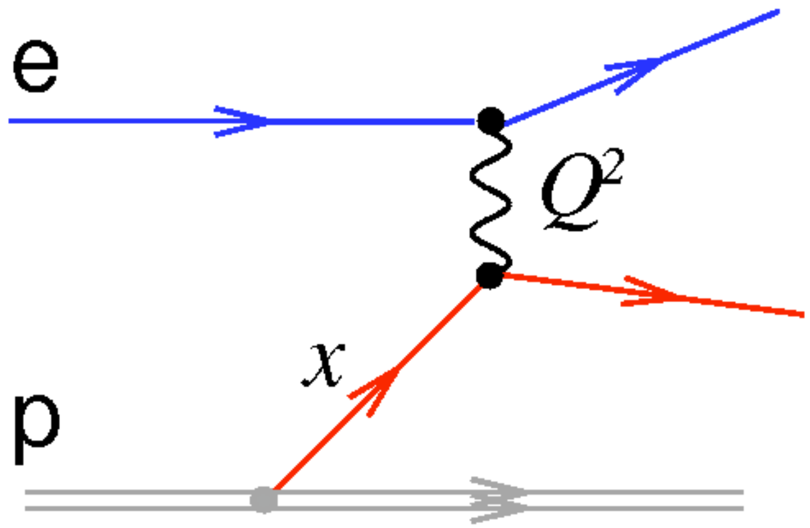

0'th order α_s

no hard QCD radiation

One jet in Lab frame

order α_s^2, NLO pQCD

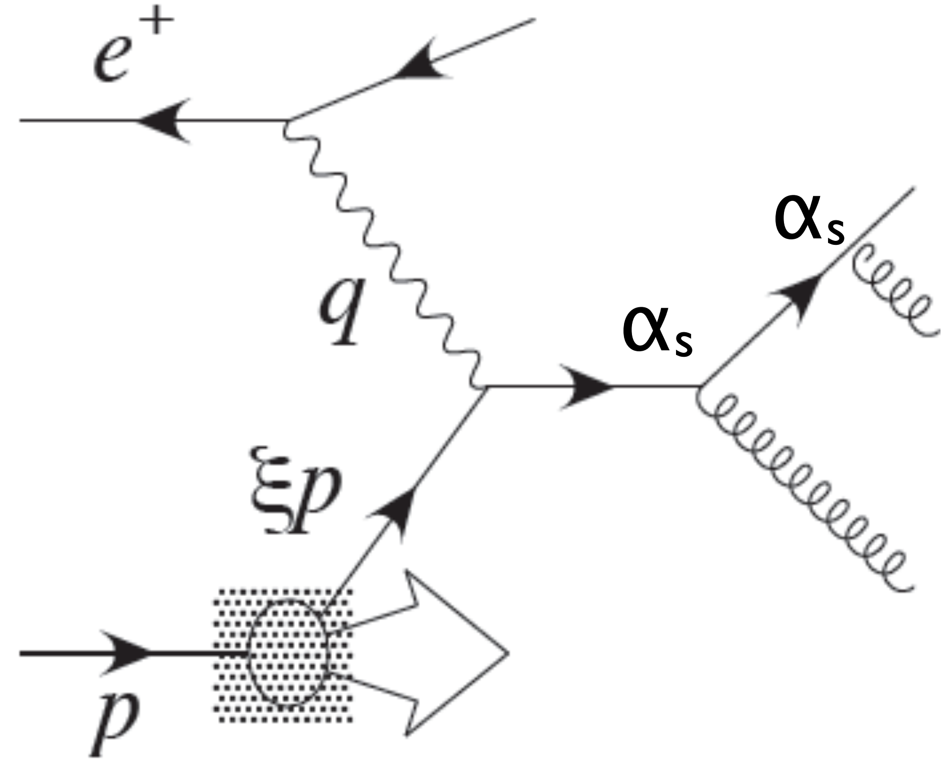

BREIT

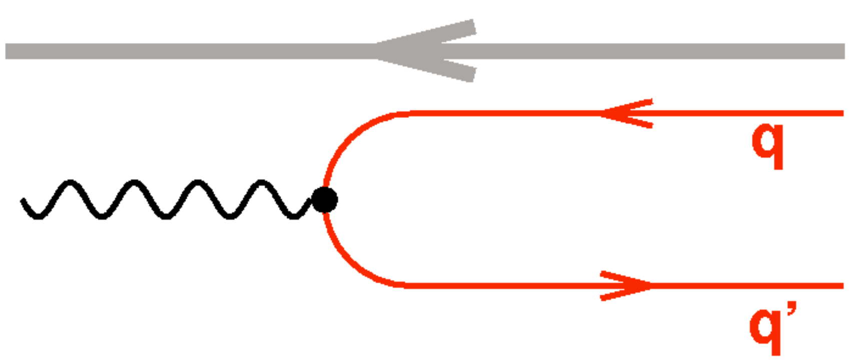

No E_T ,
No jets in Breit frame!

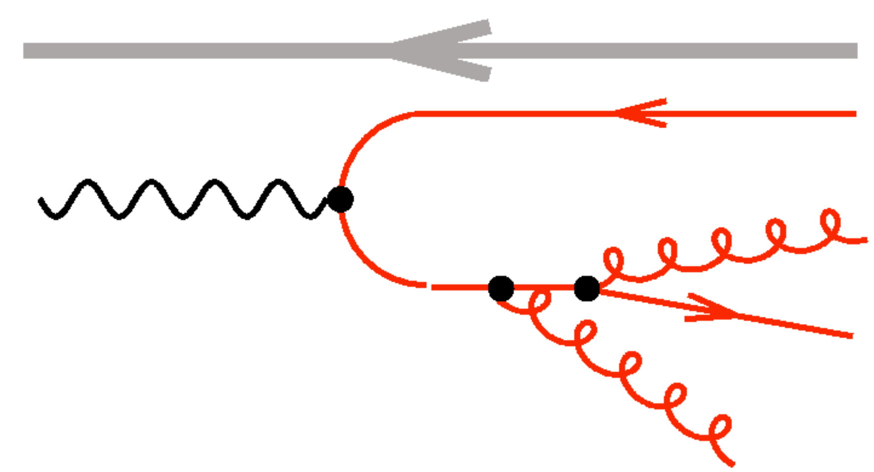

In the Breit frame, QCD radiation generates E_T

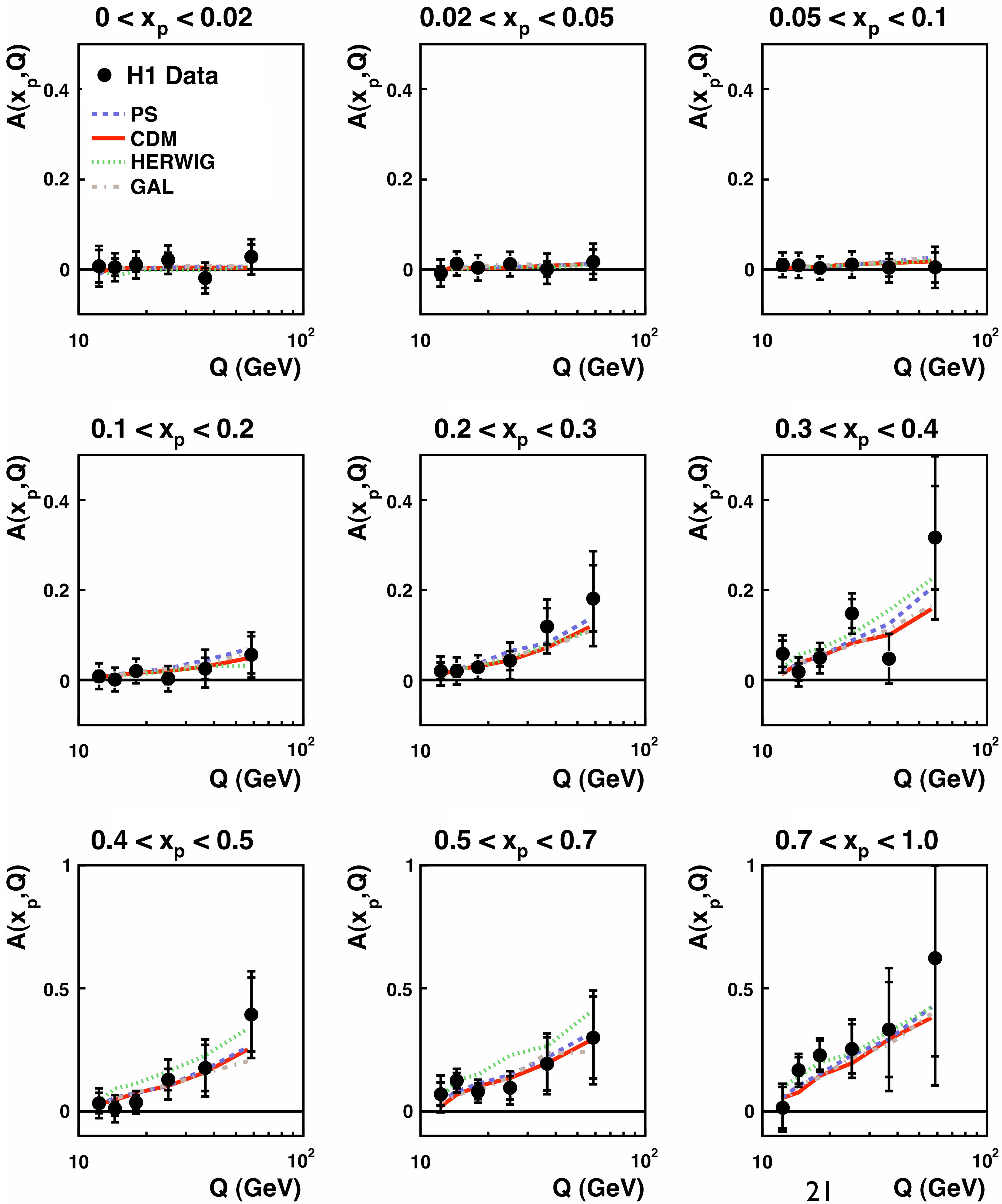

At low Q^2 (low x_{BJ}) all x_P, asymmetry ~0

As Q^2 increases asymmetry develops at high x_P, low x_P it remains ~0

Monte Carlo models are able to describe the magnitude and evolution of the asymmetry

The Gaussian fit method

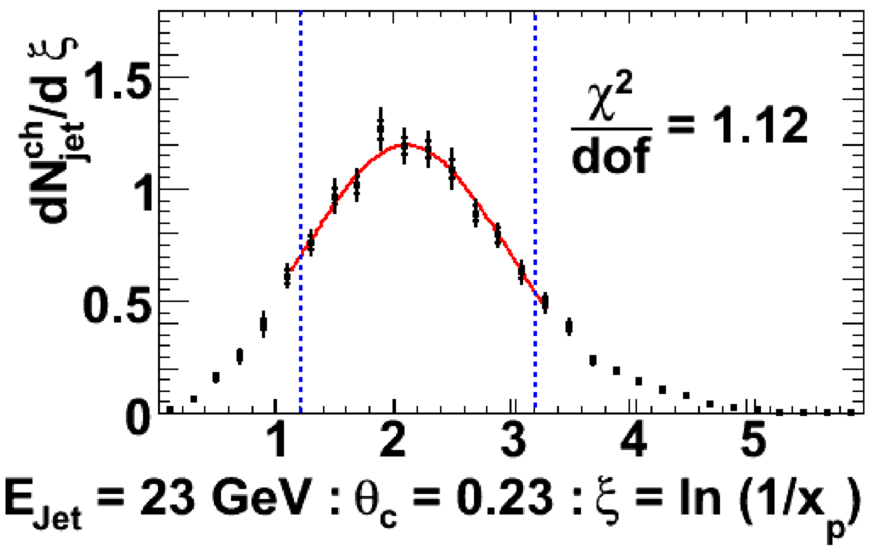

Peak position, ξ_{peak}

- Fit Gaussian ± 1 around mean.
- $\forall\ \xi$, independently measure ξ_{peak}.

$$\Lambda_{eff} = \frac{E_{Jet}\sin(\theta_c)}{e^{\left(\sqrt{0.87+2\xi_{peak}}-0.54\right)^2}} \qquad (@\ \mathrm{LO})$$

Measuring Λ_{eff}

- Only use $\theta_c = 0.23$ energy points:
  - Different θ_c values are correlated;
  - MLLA looses validity at large θ_c.
- Fit equation to all 5 energy points.

$$\Lambda_{eff} = 275 \pm 4\,(\mathrm{stat.})^{+4}_{-8}\,(\mathrm{syst.})\ \mathrm{MeV}$$

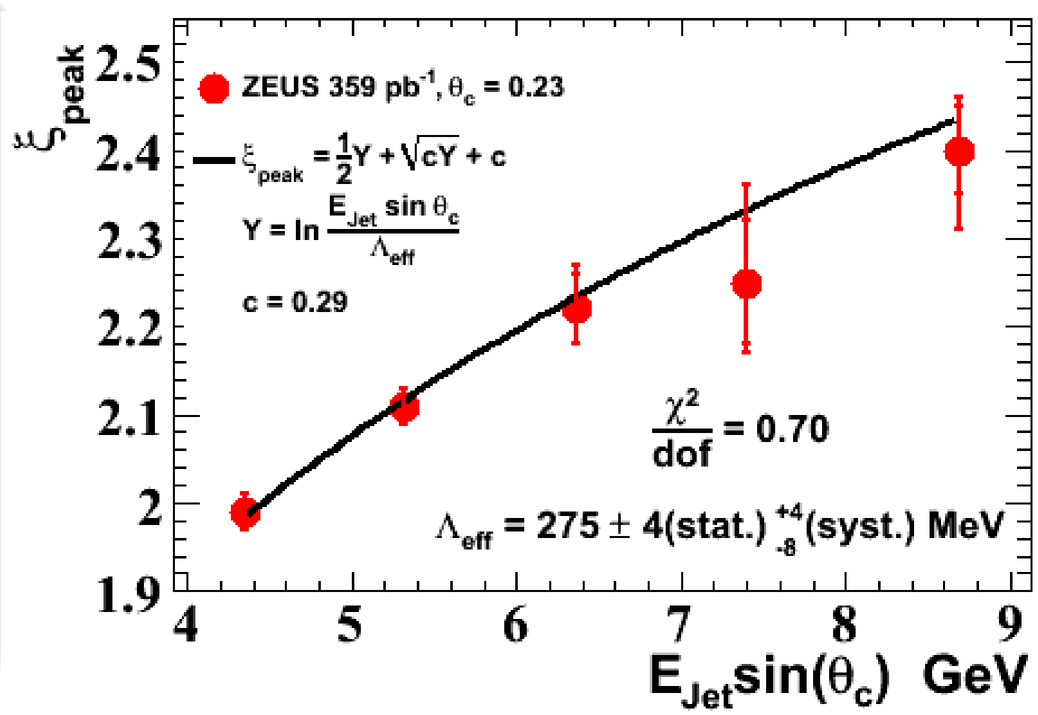

The MLLA + LPHD fit method

Momentum distribution of partons from a gluon is given by:

- $$\bar{D}^{\rm lim}_{\rm g-Jet}\left(\ln\left(\frac{1}{x_p}\right), Y\right) = \frac{4C_f}{b}\Gamma(B)\int_{-\frac{\pi}{2}}^{\frac{\pi}{2}} e^{-B\alpha}\left[\frac{\cosh\alpha+(1-2\zeta)\sinh\alpha}{\frac{4N_c}{b}Y\frac{\alpha}{\sinh\alpha}}\right]^{\frac{B}{2}}$$
  $$\cdot\, I_B\left(\sqrt{\frac{16N_c}{b}Y\frac{\alpha}{\sinh\alpha}[\cosh\alpha+(1-2\zeta)\sinh\alpha]}\right)\frac{d\tau}{\pi}$$
- Valid for: $\ln\left(\frac{1}{x_p \ll 1}\right) \leq \ln\left(\frac{1}{x_p}\right) \leq \ln\left(\frac{M_{2j}}{2P_0}\right)$ $\quad P_0 = \text{Upper bound}$

For number of flavours, $N_f = 3$, and number of colours, $N_c = 3$

- $C_f = \frac{9}{4}$, $b = 9$, $B = 1.247$.
- I_B is the modified Bessel function of order B.
- $\alpha = \alpha_0 + i\tau$, where α_0 is determined by $\tanh\alpha_0 = 2\zeta - 1$
- $\zeta = 1 - \frac{\ln\left(\frac{1}{x_p}\right)}{Y}$ and $Y = \ln\left(\frac{E_{\rm Jet}\sin(\theta_c)}{\Lambda_{\rm eff}}\right)$ $\qquad \bar{D}^{\rm lim}_{\rm q-Jet} = \frac{1}{r}\bar{D}^{\rm lim}_{\rm g-Jet}$